Transcription termination factor Rho can displace streptavidin from biotinylated RNA

Annie Schwartz, Emmanuel Margeat, A. Rachid Rahmouni, Marc Boudvillain

THE JOURNAL OF BIOLOGICAL CHEMISTRY VOL. 282, NO. 43, pp. 31469–31476, October 26, 2007

Transcription Termination Factor Rho Can Displace Streptavidin from Biotinylated RNA*

Received for publication, August 20, 2007, and in revised form, August 27, 2007 Published, JBC Papers in Press, August 27, 2007, DOI 10.1074/jbc.M706935200

Annie Schwartz[‡], Emmanuel Margeat[§], A. Rachid Rahmouni[‡], and Marc Boudvillain[‡1]

From [‡]CNRS UPR4301, Centre de Biophysique Moléculaire, Rue Charles Sadron, 45071 Orléans cedex 2, France and the [§]CNRS UMR5048, Centre de Biochimie Structurale, 29 Rue de Navacelles 34090, Montpellier, France, INSERM U554, 34090, Montpellier, France, Universités Montpellier 1 et 2, 34090 Montpellier, France

In *Escherichia coli*, binding of the hexameric Rho protein to naked C-rich *Rut* (Rho utilization) regions of nascent RNA transcripts initiates Rho-dependent termination of transcription. Although the ring-shaped Rho factor exhibits *in vitro* RNA-dependent ATPase and directional RNA-DNA helicase activities, the actual molecular mechanisms used by Rho to disrupt the intricate network of interactions that cement the ternary transcription complex remain elusive. Here, we show that Rho is a molecular motor that can apply significant disruptive forces on heterologous nucleoprotein assemblies such as streptavidin bound to biotinylated RNA molecules. ATP-dependent disruption of the biotin-streptavidin interaction demonstrates that Rho is not mechanistically limited to the melting of nucleic acid base pairs within molecular complexes and confirms that specific interactions with the roadblock target are not required for Rho to operate properly. We also show that Rho-induced streptavidin displacement depends significantly on the identity of the biotinylated transcript as well as on the position, nature, and length of the biotin link to the RNA chain. Altogether, our data are consistent with a "snow plough" type of mechanism of action whereby an early rearrangement of the Rho-substrate complex (activation) is rate-limiting, physical force (pulling) is exerted on the RNA chain by residues of the central Rho channel, and removal of structural obstacles from the RNA track stems from their nonspecific steric exclusion from the hexamer central hole. In this context, a simple model for the regulation of Rho-dependent termination based on the modulation of disruptive dynamic loading by secondary factors is proposed.

In *Escherichia coli*, a large fraction of transcription termination events require the participation of the endogenous Rho protein (1, 2). The Rho factor is a ring-shaped homohexamer (3–5) that possesses *in vitro* RNA-dependent ATPase (6) and ATP-dependent RNA and RNA-DNA helicase activities (7, 8). To induce transcription termination, Rho hexamers usually bind to characteristic C-rich/G-poor segments of the nascent transcript called *Rut*[2] (for Rho Utilization) sites from which they move directionally along the RNA chain to catch up with and ultimately dissociate the transcription elongation complex (TEC) located at the transcript 3′-end (9–18). At present, the exact mechanism by which Rho dissociates the TEC remains unknown. It has been believed for some time that the Rho helicase could directly unwind the RNA-DNA hybrid that the 3′-end of the nascent transcript forms with the DNA template within the TEC. However, recent structural data indicate that this short ~9-base pair-long RNA-DNA hybrid is too deeply buried within the TEC interior for direct helicase action (19, 20). This observation has prompted alternative models whereby the Rho enzyme, once positioned on the polymerase surface, applies NTPase-driven physical force to pull the RNA from the TEC and/or drive forward the polymerase into an hypertranslocated and unstable state (21–23). Importantly, these models imply that the RNA and RNA-DNA unwinding activities of Rho are essentially nonspecific *in vitro* byproducts of the enzyme progression along the RNA track. This proposal is reminiscent of the "snow plough"-type of mechanisms proposed for various helicases and is consistent with the emerging view of helicases being able to perform a larger set of remodeling tasks on nucleic acid (NA) and nucleoproteic assemblies than simply separating NA strands (24–26).

Rho function can be tightly regulated by transcription factors, such as NusA and NusG (27, 28), that alter the conformation of the TEC (29, 30). Although these alterations are likely to modulate the strength and/or elongation rate of the TEC, Rho may also respond differentially to specific, factor-induced, structural features of the TEC isoforms. Similarly, defects in Rho-dependent termination induced by single-point mutations of the α-C-terminal domain of the RNA polymerase (RNAP) may stem from altered Rho-RNAP contacts (31). However, the presence of specific Rho-RNAP interactions would support a mechanism slightly more elaborate than simple snow plough displacement of structural obstacles from the NA track.

Although the TEC is a macromolecular assembly that is much more complex than regular helicase substrates (*i.e.* bare NA helices), it derives a large part of its thermodynamic stability from NA base pairings (see Ref. 32 and references therein). This raises the possibility that Rho mechanochemical work may

* This work was supported by grants from the Agence Nationale de la Recherche (Grant PCV06_135253), the Association pour la Recherche sur le Cancer (Grant 3639), and the Ligue contre le Cancer (Région Centre). The costs of publication of this article were defrayed in part by the payment of page charges. This article must therefore be hereby marked "*advertisement*" in accordance with 18 U.S.C. Section 1734 solely to indicate this fact.

[1] To whom correspondence should be addressed. Tel.: 33-238-25-55-85; Fax: 33-238-63-15-17; E-mail: marc.boudvillain@cnrs-orleans.fr.

[2] The abbreviations used are: *Rut*, Rho utilization; TEC, transcription elongation complex; NA, nucleic acid; nt, nucleotide; ^{Bt}N, biotinylated nucleotide residue; RNAP, RNA polymerase; MOPS, 4-morpholinepropanesulfonic acid.

be limited to the disruption of NA pairings within molecular complexes. This proposal, however, would also not be totally consistent with a snow plough-type of mechanism since the strength rather than the chemical nature of the roadblock interactions with the NA track should impact the efficiency (processivity) of the helicase ("translocase") enzyme. To clarify these important aspects of the Rho mechanism, we have evaluated the ability of the enzyme to displace a heterologous protein from a transcript substrate. We selected the biotin-streptavidin complex as a model system because it has a number of interesting advantages to probe the Rho mechanism: a biotin moiety can be readily introduced at various positions of the RNA chain by chemical and enzymatic methods; the biotin-streptavidin interaction is stronger ($K_d \sim 10^{-13}$ M) (33, 34) than most NA-protein interactions; the spontaneous dissociation of biotin from streptavidin is significantly slower ($k_{off} \sim 3 \times 10^{-3}$ min^{-1} at 37 °C) (33, 34) than the ATP-dependent Rho dissociation activity inferred from unwinding of model RNA-DNA substrates ($k_{obs} > 0.1$ min^{-1} at 37 °C) (35–37); the biotin and streptavidin moieties are held together by interactions that differ markedly from the hydrogen bond networks involved in NA base pairs (Ref. 34 and references therein). Here, we show that Rho can displace streptavidin from biotinylated transcript substrates in an ATP-dependent fashion. This indicates that Rho activity is not very much modulated by the nature of the roadblock target. This observation is consistent with a snow plough-type of mechanism of steric exclusion of the roadblock from the central channel of the Rho hexamer (where the RNA strand is pulled in by the enzyme) (38–40). Yet, we also show that the position and nature of the chemical link of biotin to the RNA strand as well as the identity of the transcript can significantly impact the efficiency of streptavidin displacement by the Rho enzyme. These observations are in line with the idiosyncratic responses of the Rho helicase to modifications of model RNA-DNA substrates (36, 37) and suggest that the same kinetic and RNA structure factors control the NA strand and protein displacement reactions.

EXPERIMENTAL PROCEDURES

Materials—Chemicals and enzymes were obtained from Sigma-Aldrich and New England Biolabs, respectively. Oligonucleotides were purchased from Biomers.net and Dharmacon and were systematically purified by polyacrylamide gel electrophoresis (PAGE). Core streptavidin (13.3 kDa/monomer) was obtained from Promega. The Rho protein (concentrations expressed in units of hexamers throughout this report) was prepared and characterized as described previously (37, 41).

The DNA templates encoding the R_{107} and R_{132} transcripts were obtained by PCR amplification of specific regions of the pAS02 plasmid that contains the R_{157} sequence downstream from a T7 promoter (36). These templates, or the pAS02 plasmid linearized with SmaI (for the preparation of the R_{157} transcripts), were transcribed *in vitro* with T7 RNA polymerase as described previously (42) using larger reaction volumes (500 μl) and longer incubation times (2–3 h). The resulting transcripts were purified by 5–7% denaturing PAGE and stored at −20 °C in $M_{10}E_1$ buffer (10 mM MOPS, pH 6.5, 1 mM EDTA).

Preparation of the Biotinylated Transcripts—We used two distinct synthesis routes to attach biotin-derivatized linkers to various positions of *aRut* (*a*rtificial *Rut*; see Refs. 9, 36, 37) containing RNA molecules. On the one hand, the transcripts were biotinylated specifically at their 3′-ends by controlled oxidation with sodium periodate followed by coupling with EZ-link biotin hydrazides (Pierce), as described (43). On the other hand, synthetic RNA oligonucleotides containing primary amine linkers at specific positions were reacted with EZ-link biotin succinimidyl esters (Pierce). Biotinylated R_{132} molecules were then obtained by ligating these modified oligonucleotides to the 3′-ends of R_{107} transcripts using T4 RNA ligase and DNA splints, as described (44). Because neither synthesis route ensured 100% biotinylation of the RNA molecules, the correct products were selected through their ability to bind streptavidin: 10 pmol ^{32}P-labeled molecules were incubated with streptavidin (1 μM) in hybridization buffer (150 mM potassium acetate (Kac), 20 mM HEPES, pH 7.5, 0.1 mM EDTA, 0.1 mg/ml bovine serum albumin) for 15 min at 30 °C. Streptavidin-RNA complexes were then purified by 7% native PAGE (gels contained 0.3% SDS to maximize the fractions of specific complexes), eluted from the gel bands in streptavidin buffer (0.3 M KAc, 100 nM streptavidin) for 1.5 h at 30 °C, and precipitated with 3 volumes of ethanol before being stored at −20 °C in helicase buffer (150 mM KAc, 20 mM HEPES, pH 7.5, 0.1 mM EDTA, 0.1 mM dithiothreitol). The amounts of byproducts (such as complexes containing more that one RNA strand/streptavidin tetramer or biotinylated RNA strands bound to streptavidin dimers) were substantially reduced (<10%) with this procedure. However, it is possible that a small fraction of the biotinylated RNA-streptavidin complexes evolve into an unstable population (see "Results") during the elution step. The RNA concentrations were determined by UV measurements with a μl-spectrophotometer (Nanodrop) and/or from specific activities of the samples. The DINAmelt server (45) was used to predict the secondary structures of the RNA constructs.

Streptavidin Displacement Reactions—Purified streptavidin-RNA complexes (~1 nM, final concentration) were mixed with Rho hexamers (20 nM) in helicase buffer and incubated for 3 min at 30 °C. The displacement reaction was initiated with a mixture of ATP, $MgCl_2$ (1 mM, final concentrations), and free biotin (10 μM, final concentration). Reaction aliquots were taken at various times, mixed with 3 volumes of quench buffer (150 mM Kac, 20 mM HEPES, pH 7.5, 26 mM EDTA, 0.4% SDS, 5% Ficoll-400), and immediately loaded on a 6% polyacrylamide gel containing 0.3% SDS to selectively denature Rho-RNA complexes. All displacement reactions were performed at least in triplicate but could not be repeated under single-turnover conditions because poly[rC], which is used as the Rho trap (35–37), had a dose-dependent inhibitory effect on Rho-induced dissociation of the RNA-streptavidin complexes (data not shown; peculiar poly[rC] effects have also been observed in other circumstances; see Refs. 37, 46). Detection and quantification of gel bands were performed with a Storm-860 imager and related software (GE Healthcare). The fractions of individual products present in the reaction at a given time were determined with the following formula, $F_t = (I_t - F_0 \times \Sigma I_{i,t})/((1 - F_0) \times \Sigma I_{i,t})$ (with $F_0 = I_0/\Sigma I_{i,0}$), where I_0 and I_t are the intensities of the product

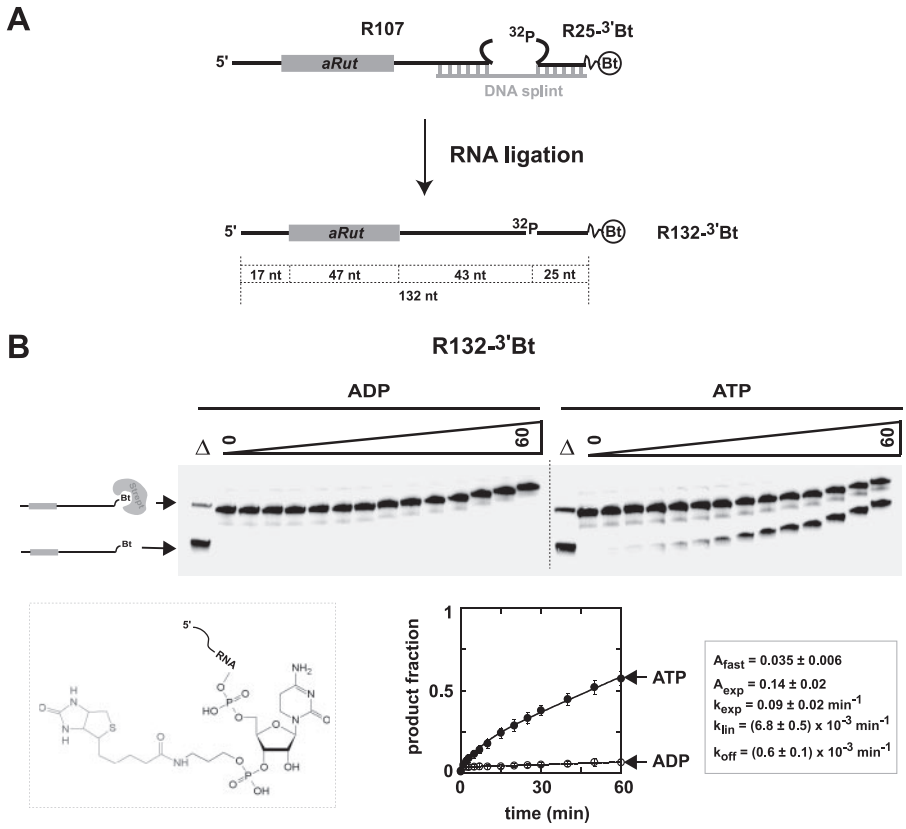

FIGURE 1. **Rho-induced dissociation of streptavidin from a biotinylated transcript substrate.** *A*, schematic of the "splint-directed" ligation strategy that was used to prepare the biotinylated R132-$^{3'}$Bt and R132-U^{8}Bt substrates from 107-nt RNA transcripts and biotin-derivatized oligoribonucleotides. The case of the R132-$^{3'}$Bt substrate is provided as an example. The R107 transcript contains the short *aRut* sequence that is sufficient to promote a functional interaction with the Rho enzyme (9, 37). The sizes, in nucleotides, of the relevant RNA regions are indicated below the diagram of the R132-$^{3'}$Bt substrate. *B*, active displacement of streptavidin from the R132-$^{3'}$Bt substrate. The R132-$^{3'}$Bt-Streptavidin complexes (5 nM) were preincubated for 3′ at 30 °C with an excess of Rho hexamers (20 nM). The displacement reaction was then initiated with a mix of $MgCl_2$ (1 mM), ATP (1 mM), and biotin (10 μM). In control experiments, ATP was replaced by ADP. At various times (reaction timeframes are depicted schematically, in min, above the gel lanes), aliquots were removed from the helicase mixtures, mixed with quench buffer, and loaded immediately on a 6% polyacrylamide gel containing 0.3% SDS to selectively denature Rho-NA complexes (Ref. 37 and data not shown). *Lanes* Δ correspond to heat-denatured reaction aliquots. To account for complex reaction kinetics under ATP conditions, the experimental data points were fitted with Kaleidagraph (Synergy Software) using various equations describing alternative mechanisms. Best fits ($R^2 > 0.98$) were obtained with the equation: $y = A_{fast}(1 - e^{-(k^t_{fast})}) + A_{exp}(1 - e^{-(k^t_{fast})}) + k_{lin}t$. This equation describes a pre-steady state regimen for the ATP-dependent reaction (35, 37) as well as a small ATP-independent pseudo first-order reaction burst (A_{fast}, k_{fast}). Because reaction aliquots cannot be collected manually at times below ~20 s, k_{fast} could not be accurately determined and was arbitrarily set to 10 min^{-1}. The rates of first-order decay of the botinylated RNA-streptavidin complexes (k_{off}) measured under ADP conditions (*left gel*) were derived from data fitting to the following equation: $y = A_{fast}(1 - e^{-(k^t_{fast})}) + (1 - A_{fast})(1 - e^{-(k^t_{off})})$. The values obtained for A_{fast} under ATP and ADP conditions agreed well. The chemical attachment of biotin to the 3′-end of the RNA substrate is depicted in the *inset*.

bands after incubation of the helicase reaction for 0 or t min at 30 °C, respectively ($\Sigma I_{i,0}$ and $\Sigma I_{i,t}$ are the sums of the intensities of the bands per gel lane measured under the same respective conditions). Note that $F_0 < 0.05$ in most experiments.

RESULTS

Rho Can Disrupt a Biotin-Streptavidin Complex Linked to the 3′-End of an RNA Substrate—To probe the capacity of the Rho enzyme to disrupt the biotin-streptavidin interaction, we have used 132-nucleotide (nt)-long RNA constructs containing a synthetic Rho loading site (*aRut* sequence; see Refs. 9, 36, 37, 46 for the characterization of *aRut*) upstream from a biotinylated nucleotide (^{Bt}N) residue that were obtained by splint-directed RNA ligations (Fig. 1*A*) (44). To avoid potential interference of the biotin-streptavidin complex with the formation of a productive Rho-RNA complex (36), a large distance (>60 nt) was set initially between the *aRut* site and a 3′-terminal ^{Bt}N residue (R132-$^{3'}$Bt construct; Fig. 1*A*). In a first series of experiments, ^{32}P-labeled R132-$^{3'}$Bt constructs were mixed with core streptavidin (this mature form lacks the C-terminal polypeptide domain that can compete for the biotin binding site) (47), and the resulting complexes were purified by PAGE (see "Experimental Procedures"). The RNA-streptavidin complexes were then incubated with Rho for 3 min at 30 °C before addition of an initiation mixture containing ATP, $MgCl_2$, and an excess of biotin (to trap free streptavidin molecules). Reaction aliquots were removed at various times and immediately loaded on a native (with respect to NA species) gel containing 0.3% SDS (in these electrophoretic conditions, Rho-RNA complexes are selectively denatured; data not shown). The spontaneous release of core streptavidin from the biotinylated transcripts was also monitored in control experiments containing ADP instead of ATP. As shown in Fig. 1*B* (*ADP lanes* and *graph*), this reaction is very slow with the R132-$^{3'}$Bt-streptavidin complexes ($k_{off} \sim 0.6 \times 10^{-3}$/min at 30 °C), which is in good agreement with published work on the biotin-streptavidin interaction ($k_{off} \sim 3 \times 10^{-3}$/min at 37 °C) (33, 34). However, dissociation of the R132-$^{3'}$Bt-streptavidin complexes was dramatically accelerated under conditions promoting Rho helicase activity (Fig. 1*B*, *ATP lanes*). This effect was strictly dependent on the presence of Rho, $MgCl_2$, and excess biotin in the reaction mixture and was inhibited by pairing of a complementary oligonucleotide to the *aRut* sequence (data not shown). Altogether, these data are consistent with the active displacement of streptavidin from the R132-$^{3'}$Bt transcript promoted by the Rho enzyme.

The kinetic profile of the streptavidin displacement reaction is complex, probably reflecting distinct reaction phases and pathways (Fig. 1*B*, *graph*). On the one hand, a small fraction ($A_{fast} < 5\%$) of the RNA-streptavidin complexes were quickly dissociated ($k_{fast} \geq 10$ min^{-1}) in an ATP-independent fashion. This minor reaction was unaffected by the presence of nonspecific competitors (bovine serum albumin or tRNA) in the mix-

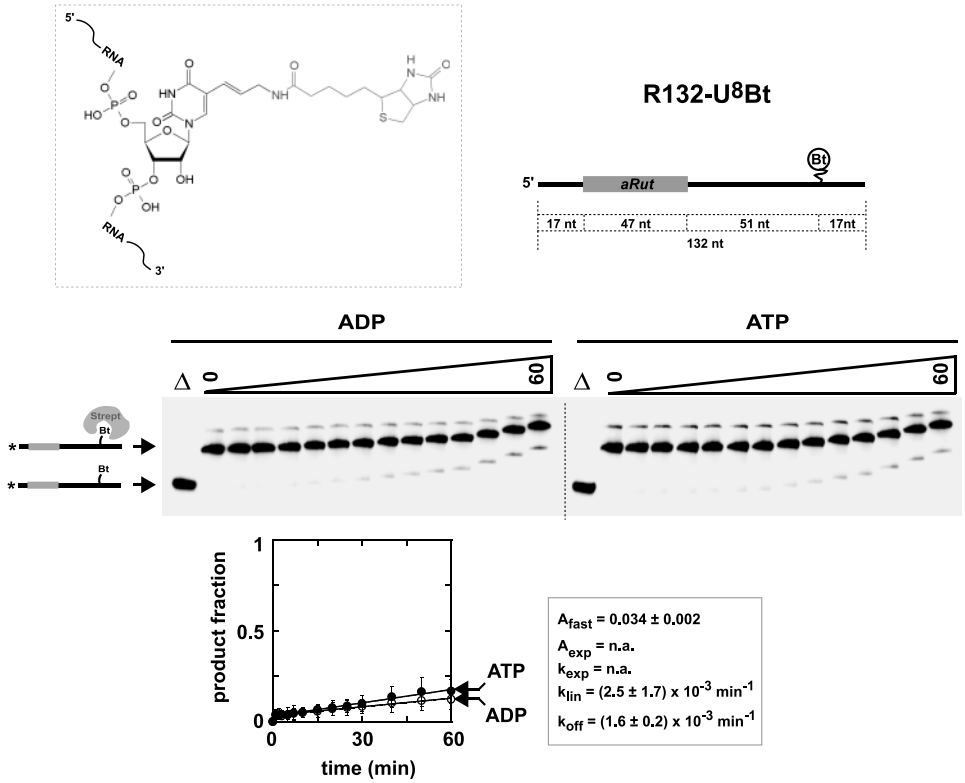

FIGURE 2. **Streptavidin bound to the R132-U^{8}Bt substrate is not actively displaced by Rho.** The R132-U^{8}Bt substrate contains a biotin moiety linked to the pyrimidine ring of the internal U^{115} residue (*inset* and *diagram*). Streptavidin displacement was assayed at 30 °C under standard multirun conditions as described in the legend to Fig. 1.

ture, the absence of the Rho enzyme, or the lack of SDS in the gel (in control reactions without Rho) but required biotin in the initiation mix (data not shown). On the other hand, most RNA-streptavidin complexes (>95%) were actively dissociated by the Rho enzyme in two distinct ATP-dependent reaction phases (Fig. 1*B*), mimicking the pre-steady state profiles of multirun Rho helicase reactions (35, 37). From this analogy, one can speculate that streptavidin is removed from ~15% of the RNA substrates during the first Rho translocation run (exponential phase; A_{exp}, k_{exp}). This, in turn, suggests that the first run is unproductive for a significant fraction of the initial Rho-substrate complexes (*i.e.* Rho dissociates from the substrates before being able to displace streptavidin). However, streptavidin is also actively displaced from the complexes during subsequent Rho turnovers with an efficiency that is probably similar to the first run (~15%) and at a rate (linear phase, $k_{lin} \sim 7 \times 10^{-3}$/min) that remains higher than for spontaneous dissociation of streptavidin ($k_{off} \sim 0.6 \times 10^{-3}$/min, ADP conditions).

The Efficiency of Streptavidin Displacement Depends on the Position of Biotin Attachment to the RNA Substrate—The data presented above demonstrate that the ATPase-fueled mechanochemical work of the Rho enzyme is not restricted to the disruption of NA pairing interactions. Yet, the fraction of R132-$^{3'}$Bt-streptavidin complexes that are dissociated in a single Rho enzymatic run does not seem very high (~15%, Fig. 1*B*), especially when compared with the amplitude of single-turnover RNA-DNA helicase reactions (36, 37). This moderate efficiency of the Rho motor may be due to the nature of the biotin-streptavidin interaction or, alternatively, to the position of the streptavidin roadblock at the 3′-end of the RNA chain. To evaluate these possibilities, we have prepared another substrate in which the ^{Bt}N residue is located at an internal position of the RNA chain (R132-U^{8}Bt; Fig. 2, *inset*). Rho displacement reactions were performed with R132-U^{8}Bt-streptavidin complexes under the experimental conditions described above. In this case, however, Rho could not actively displace streptavidin from the biotinylated RNA substrate (Fig. 2). Thus, the displacement efficiency of the Rho enzyme depends on the position of biotin attachment to the RNA chain (note, however, that Rho can displace a DNA oligonucleotide hybridized to the 110–132 region of the R132-U^{8}Bt substrate with normal helicase efficiency; data not shown).

The formation of a productive Rho-RNA complex, the likely crucial rate-limiting step during *in vitro* RNA-DNA helicase reactions, is sensitive to the local steric environment (36). We therefore wondered whether structural hindrance due to the binding of a bulky streptavidin tetramer closer to the Rho loading site could account for the loss of streptavidin displacement activity with the R132-U^{8}Bt substrate. To test this hypothesis, we introduced a biotin moiety at the 3′-end of the R107 transcript (R107-$^{3'ox}$Bt substrate; see "Experimental Procedures"), thereby generating an 8-nt shorter distance between the ^{Bt}N residue and the *aRut* site than in R132-U^{8}Bt. Interestingly, Rho actively displaced streptavidin from R107-$^{3'ox}$Bt (Fig. 3*A*), which rules out a simple distance effect to explain the absence of Rho activity with R132-U^{8}Bt (Fig. 2). Because the displacement reaction was moderately efficient with the R107-$^{3'ox}$Bt substrate, we also tested longer RNA substrates bearing the same biotin linker at their 3′-end (R132-$^{3'ox}$Bt and R157-$^{3'ox}$Bt substrates). Although Rho-induced displacement of streptavidin was improved significantly with R132-$^{3'ox}$Bt (with an efficiency per enzyme run now comparable with NA unwinding reactions), it was not better with the longer R157-$^{3'ox}$Bt substrate (Fig. 3*B*). From these data, it appears that the position of the ^{Bt}N residue within the RNA chain rather than its mere distance to the *aRut* site (a minimal spacer of single-stranded RNA is likely required, however; see Ref. 36) affects the streptavidin displacement reaction triggered by Rho. Variations in the reaction efficiency upon small changes of the RNA sequence that might affect the secondary structure in the vicinity of the ^{Bt}N residue (data not shown) suggest that the RNA fold may be an important factor. However, factors such as the length of the RNA chain or how biotin is attached to the RNA (*i.e.* internally or at the 3′-end) may also contribute significantly to the differences in reactivity.

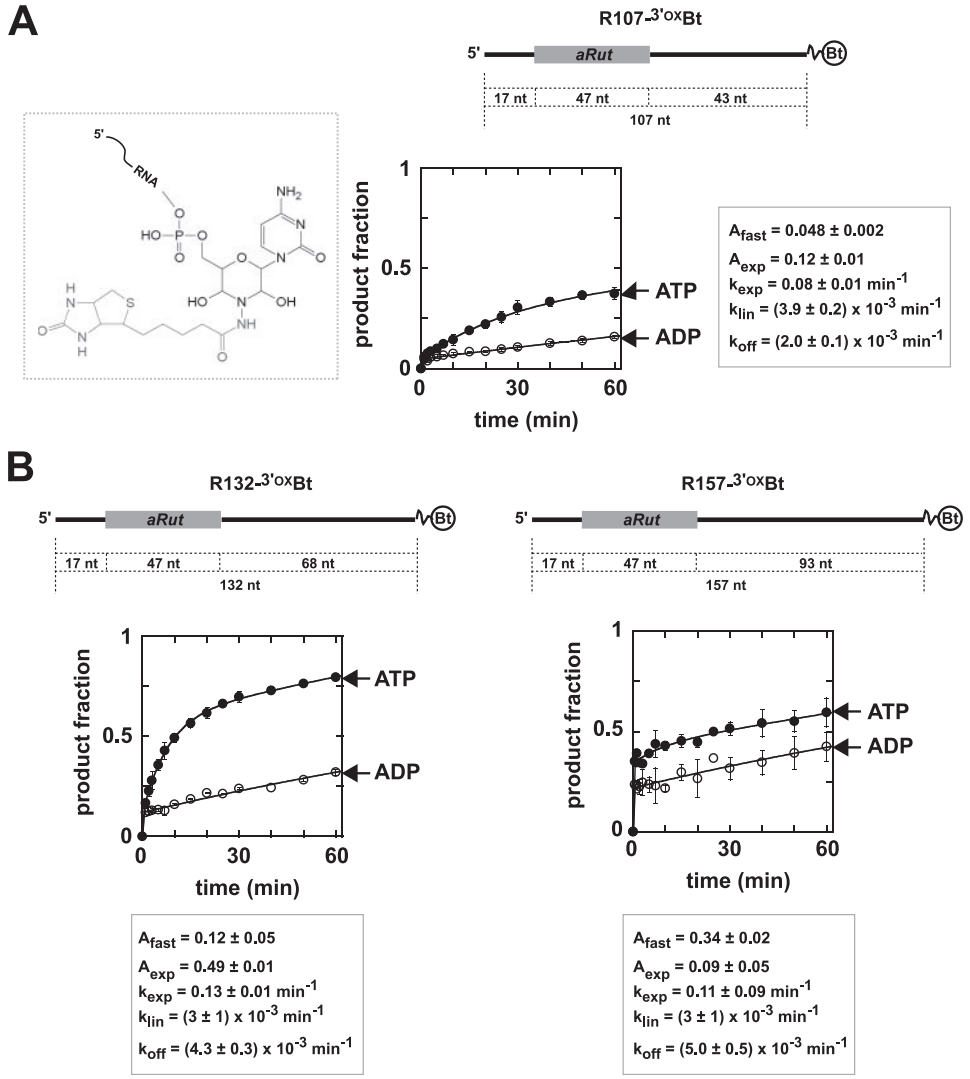

FIGURE 3. **Rho-induced dissociation of streptavidin from 3′-end biotinylated substrates that are 107 (*A*) or 132 and 157 (*B*) nt long.** The biotin moieties were linked to the oxidized 3′-ends of the RNA molecules via a hydrazone bond as depicted schematically in *panel A* (*inset*). Experiments were performed and analyzed as described in the legend to Fig. 1.

Moreover, we note that the amplitude of the ATP-independent side reaction (A_{fast}) and the rate of spontaneous dissociation (k_{off}), two Rho-independent features, somewhat vary with the biotinylated substrate (Figs. 1–3). This suggests that subtle variations in the structure and/or strength of the biotin-streptavidin complex may also contribute to the observed differences in Rho efficiency.

Spatial Limitations on Rho Dissociation Activity—We have shown that Rho can actively dissociate streptavidin molecules bound to the 3′-end of biotinylated RNA substrates (Figs. 1*B* and 3). This indicates that, as for NA unwinding (36), all of the Rho contacts to the RNA chain that are necessary for productive interaction and dissociation activity are made upstream from the location of the roadblock target. This property in turn offers a good opportunity to estimate the spatial boundary for Rho action. In effect, by altering the length of the biotin linkage, one can easily change the spacing between the location of productive Rho-RNA interactions (*i.e.* where pulling on the RNA chain occurs) and the point where Rho eventually applies force on streptavidin. We thus prepared the R132-$^{3'ox:LC}$Bt substrate, which is identical to R132-$^{3'ox}$Bt excepted for the biotin spacer arm, which is ~10 Å longer (Fig. 4*A*, *inset*). This first modification had little effect on the ATP-dependent streptavidin displacement reaction (compare Fig. 3*B*, *left*, with Fig. 4*A*). When the spacer length was increased by another ~10 Å (R132-$^{3'ox:PEG4}$Bt substrate), however, Rho could no longer displace streptavidin (Fig. 4*B*). Thus, the spatial register for productive Rho action probably does not exceed ~20 Å from the point of downstream Rho interaction with cognate RNA residues. This is significantly less than the minimal distance (≥50 Å) between the Rho primary interaction subsites and the solvent-exposed surface on the opposite (downstream) side of the hexamer ring (Fig. 4*C*) (5). If one assumes that the RNA substrate traverses the central Rho channel (48) and that streptavidin dissociation occurs on the downstream side of the hexamer (streptavidin being too bulky to enter the central Rho channel), then the data imply that productive Rho-RNA contacts are formed inside the central channel of the enzyme (Fig. 4*C*). This agrees well with current biochemical and structural information and models whereby mechanochemical work (pulling) of Rho on the RNA strand is mediated by mobile side chains within the central channel of the enzyme (5, 21, 38, 39, 49).

DISCUSSION

Previous studies have shown that transcription termination factor Rho from *E. coli* can remove NA strands annealed to a transcript substrate using ATP hydrolysis as an energy source (helicase activity) (7, 8, 35–37, 50–52). We now show that mechanochemical work of Rho is not limited to the melting of NA pairings, as the enzyme can also actively dissociate streptavidin from a biotinylated RNA substrate in an ATPase-dependent fashion. This process is mediated by productive Rho-RNA contacts that form within the central channel of the Rho hexamer less than 20 Å from the point where disruptive force is applied on the streptavidin-biotin complex (Fig. 4*C*). Furthermore, streptavidin dissociation occurs with an efficiency (up to ~50%/enzyme run) and at a rate (k_{exp} ~ 0.1 min^{-1} at 30 °C) that are comparable with the ones of Rho-mediated unwinding of *aRut*-containing RNA-DNA constructs (36, 37) or dissocia-

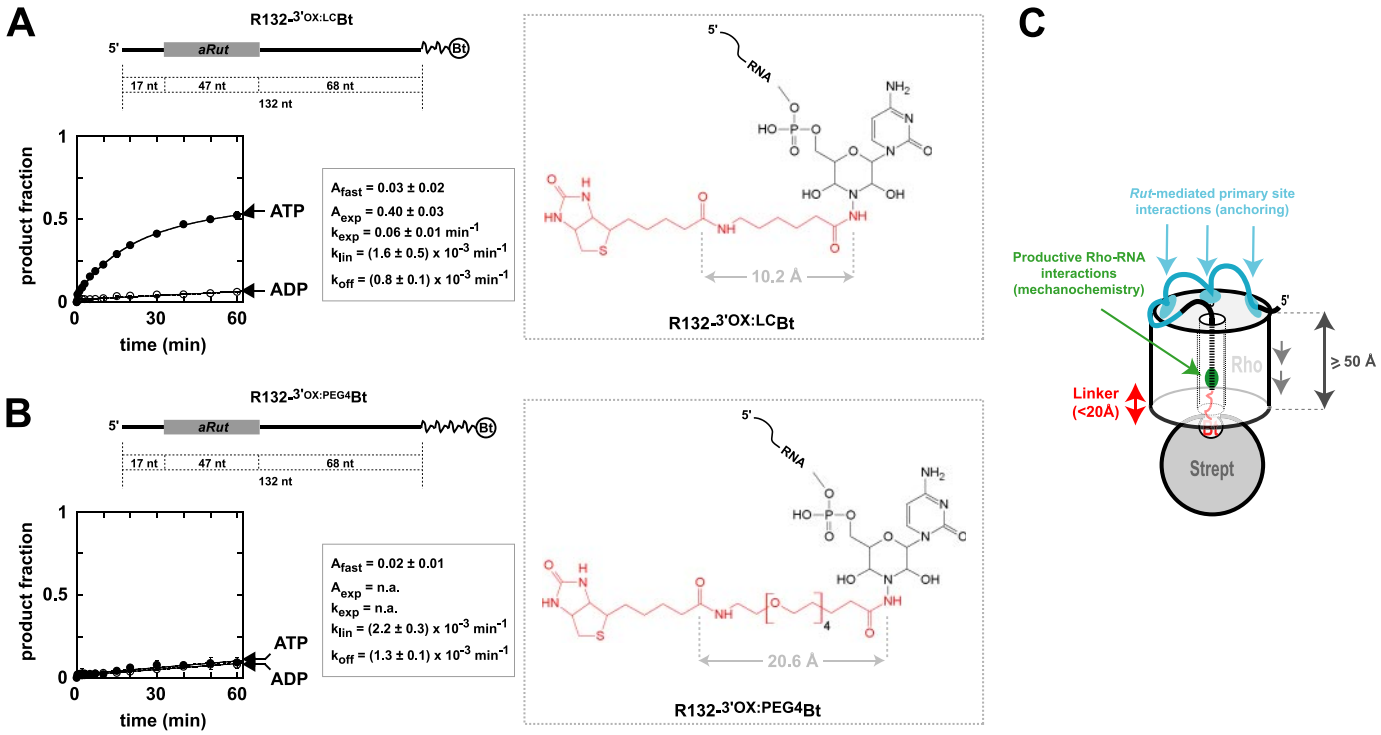

FIGURE 4. **Effect of the length of the biotin spacer arm on the streptavidin displacement reaction.** The biotinylated RNA substrates obtained after controlled oxidation of the 3′-terminal ribose and coupling with Biotin-LC (*A*) and Biotin-PEG4 (*B*) hydrazides are depicted schematically in the *insets*. *C*, schematic representation of the topology of the complex between a Rho hexamer, an RNA molecule bearing a biotin linkage at its 3′-end, and streptavidin.

tion of TECs stalled on various DNA templates (22, 53, 54). Overall, this model "RNPase" activity is a direct demonstration of the general capacity of the Rho enzyme to dissociate components that are not covalently linked to the 3′-end of the RNA (1). Similar displacement activities have been previously evidenced for DNA and RNA helicases having various biological roles and functional oligomeric states (25, 26). Thus, Rho is not unique in its ability to displace roadblocks of various kinds from an NA track nor is this ability specific to the quaternary structure, substrate preference (*i.e.* RNA *versus* DNA), or biological function of the enzyme. On the other hand, the fact that Rho can break various kinds of interactions (NA pairings, biotin-streptavidin) with similar efficiencies supports a snow plough-type of mechanism of action in which no specific interactions with the obstacle to be displaced are required. In this class of mechanisms, the enzyme interacts specifically with and tracks directionally on a single NA strand and in the process can disrupt nonspecifically intervening obstacles such as hybridized NA strands or bound proteins (55). Substrate requirements are therefore intrinsically limited to the tracking strand and usually include the presence of a small portion of single-stranded NA that serves as the initial helicase binding site as do *Rut* loading sites for Rho hexamers (48).

One way to regulate a snow plough molecular machine is through interference with (or facilitation of) the formation of a competent enzyme-NA complex. In the case of Rho, such a scenario has been recently highlighted *in vivo* with substrate variants of the λtR1 terminator (56). Regulation of Rho function at the level of the formation of a productive enzyme-NA complex may be also facilitated by kinetic control at this early stage (36). Interestingly, similar kinetic profiles for the ATP-dependent streptavidin displacement and NA unwinding reactions (see "Results" and Refs. 36, 37) suggest that, at least in our standard *in vitro* conditions, the kinetic regimen (with a rate-limiting activation step) does not change with the nature of the object to be displaced. It follows that a maximal k_{exp}/k_{off} ratio of ~150 (Fig. 1*B*) is probably much less than the actual rate enhancement of streptavidin displacement by the Rho enzyme (if activation of the Rho-substrate complex is rate-limiting, then $k_{exp} = k_{activation} \ll k_{strept\ dissociation[ATP]}$). This uncertainty, in turn, precludes a direct estimation of the disruptive force exerted by Rho on the biotin-streptavidin interaction. Early atomic force microscopy measurements yielded a bond rupture (dissociation) force of ~200 pN for the biotin-streptavidin pair (57, 58). The potential ability of Rho to develop high dissociation forces appears consistent with its biological role if one considers that forces up to 30 pN were not sufficient to mechanically pull RNA from the TEC during single-molecule experiments with laser optical tweezers (59). However, one should also note that, under non-equilibrium conditions, dissociation forces (and interaction lifetimes) can greatly vary with the force loading rate (60, 61). This parameter may therefore contribute to regulate Rho-dependent termination late on the termination pathway. Indeed, the inherently distinct energy landscapes of the Rho and TEC dissociation pathways should generate different dissociation force *versus* loading rate relationships (Fig. 5) (60, 61). It follows that, depending on dynamic loading, one nucleoproteic complex may be easier to brake than the other, which could in turn modulate termination efficiency (Fig. 5). Although probably too simplistic, this scenario may nonetheless contribute to explain NusG effects at certain Rho-dependent terminators (27, 28). Indeed, by physically connect-

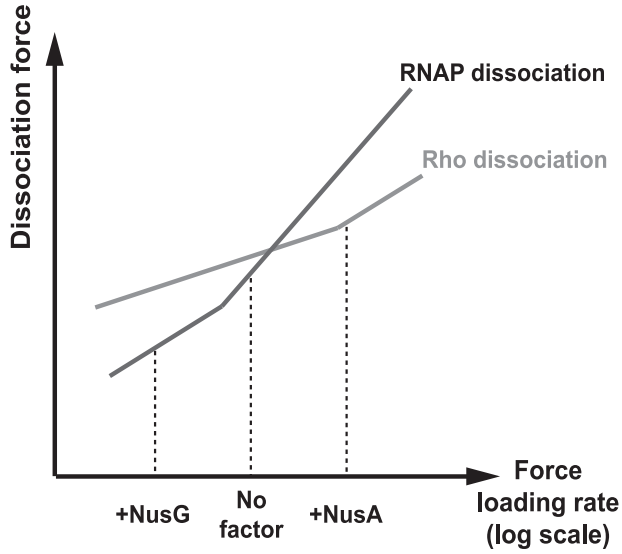

FIGURE 5. **Postulated effect of dynamic force loading on termination efficiency.** Under non-equilibrium conditions, the strengths and lifetimes of intermolecular interactions depend on the loading rate of the dissociation forces that are applied to disrupt molecular pairs (reviewed in Ref. 60). The force *versus* log (loading rate) profiles reflect the energy landscapes of the dissociation pathways along the direction of the dissociation forces; each linear region in the profile describes a sharp activation barrier at a fixed location along the dissociation pathway (60). For the purpose of discussion, the strength spectra of Rho and RNAP are represented as simple non-equivalent combinations of two linear regimes with ascending slopes. We emphasize, however, that these profiles do not describe the real dissociation processes, which are expected to be much more complicated (and hard to model), in the context of motor-driven dissociations (60). Moreover, it is important to note that the Nus factors may not only affect force loading rates as modeled but could also directly modify the Rho and RNAP dissociation pathways (not shown).

ing Rho and the RNAP (62, 63), a "spring-like" NusG (64) may cushion their intermolecular encounter (thus, reducing dynamic loading), increase the timeframe of Rho action, and thus favor RNA dissociation from the TEC at smaller dissociation forces (Fig. 5). Conversely, NusA-induced slowing of the TEC (28) may trigger a more violent intermolecular collision (and higher loading rate) and favor Rho release over TEC dissociation (Fig. 5). Of course, other factors such as the lateral stability of the TEC at pause sites (22, 65) or the probability of Rho-TEC encounter (classical kinetic competition model) (66) may also contribute significantly to the termination efficiency and are likely to become predominant in some cases (as, for instance, when NusA favors termination) (28). Further work is in progress to examine these various aspects in detail.

In summary, our results support that Rho-dependent termination of transcription stems from a snow plough-type of mechanism of steric exclusion of the TEC from the central channel of the Rho hexamer. Basal termination efficiency, however, may be significantly altered early on the termination pathway by factors impacting a productive Rho-RNA interaction (RNA conformation, steric hindrance) or at later stages by factors modulating the intermolecular collision and/or the respective strengths of the Rho-RNA and TEC complexes (collision probability, RNAP and Rho translocation rates, force distributions, and loading rates). Whether the specific RNAP mutations that alter Rho-dependent termination (31) fall in the later category awaits further work.

Acknowledgments—We gratefully acknowledge J. P. Richardson and P. H. von Hippel for the gift of materials as well as T. Bizebard for critical reading of the manuscript and helpful suggestions.

REFERENCES

1. Richardson, J. P., and Greenblatt, J. F. (1996) in *Escherischia coli and Salmonella: Cellular and Molecular Biology* (Neidhardt, F., Curtiss, R. I., Ingraham, J., Lin, E., Low, K., Magasanik, B., Reznikov, W., Riley, M., Schaechter, M., and Umbarger, H., eds) pp. 822–848, ASM Press, Washington D.C.
2. Ciampi, M. S. (2006) *Microbiology* **152,** Pt. 9, 2515–2528
3. Gogol, E. P., Seifried, S. E., and von Hippel, P. H. (1991) *J. Mol. Biol.* **221,** 1127–1138
4. Skordalakes, E., and Berger, J. M. (2003) *Cell* **114,** 135–146
5. Skordalakes, E., and Berger, J. M. (2006) *Cell* **127,** 553–564
6. Lowery-Goldhammer, C., and Richardson, J. P. (1974) *Proc. Natl. Acad. Sci. U. S. A.* **71,** 2003–2007
7. Brennan, C. A., Dombroski, A. J., and Platt, T. (1987) *Cell* **48,** 945–952
8. Brennan, C. A., Steinmetz, E. J., Spear, P., and Platt, T. (1990) *J. Biol. Chem.* **265,** 5440–5447
9. Guerin, M., Robichon, N., Geiselmann, J., and Rahmouni, A. R. (1998) *Nucleic Acids Res.* **26,** 4895–4900
10. Richardson, L. V., and Richardson, J. P. (1996) *J. Biol. Chem.* **271,** 21597–21603
11. Morgan, W. D., Bear, D. G., Litchman, B. L., and von Hippel, P. H. (1985) *Nucleic Acids Res.* **13,** 3739–3754
12. Chen, C. Y., Galluppi, G. R., and Richardson, J. P. (1986) *Cell* **46,** 1023–1028
13. Ceruzzi, M. A., Bektesh, S. L., and Richardson, J. P. (1985) *J. Biol. Chem.* **260,** 9412–9418
14. Hart, C. M., and Roberts, J. W. (1991) *J. Biol. Chem.* **266,** 24140–24148
15. Alifano, P., Rivellini, F., Limauro, D., Bruni, C. B., and Carlomagno, M. S. (1991) *Cell* **64,** 553–563
16. Zalatan, F., Galloway-Salvo, J., and Platt, T. (1993) *J. Biol. Chem.* **268,** 17051–17056
17. Zalatan, F., and Platt, T. (1992) *J. Biol. Chem.* **267,** 19082–19088
18. Hart, C. M., and Roberts, J. W. (1994) *J. Mol. Biol.* **237,** 255–265
19. Vassylyev, D. G., Vassylyeva, M. N., Perederina, A., Tahirov, T. H., and Artsimovitch, I. (2007) *Nature* **448,** 157–162
20. Cramer, P. (2002) *Curr. Opin. Struct. Biol.* **12,** 89–97
21. Richardson, J. P. (2003) *Cell* **114,** 157–159
22. Park, J. S., and Roberts, J. W. (2006) *Proc. Natl. Acad. Sci. U. S. A.* **103,** 4870–4875
23. Richardson, J. P. (2006) *Mol. Cell* **22,** 711–712
24. von Hippel, P. H. (2004) *Nat. Struct. Mol. Biol.* **11,** 494–496
25. Jankowsky, E., and Bowers, H. (2006) *Nucleic Acids Res.* **34,** 4181–4188
26. Mackintosh, S. G., and Raney, K. D. (2006) *Nucleic Acids Res.* **34,** 4154–4159
27. Sullivan, S. L., and Gottesman, M. E. (1992) *Cell* **68,** 989–994
28. Burns, C. M., Richardson, L. V., and Richardson, J. P. (1998) *J. Mol. Biol.* **278,** 307–316
29. Artsimovitch, I., and Landick, R. (2000) *Proc. Natl. Acad. Sci. U. S. A.* **97,** 7090–7095
30. Toulokhonov, I., Artsimovitch, I., and Landick, R. (2001) *Science* **292,** 730–733
31. Kainz, M., and Gourse, R. L. (1998) *J. Mol. Biol.* **284,** 1379–1390
32. Tadigotla, V. R., O'Maoiléidigh, D., Sengupta, A. M., Epshtein, V., Ebright, R. H., Nudler, E., and Ruckenstein, A. E. (2006) *Proc. Natl. Acad. Sci. U. S. A.* **103,** 4439–4444
33. Howarth, M., Chinnapen, D. J., Gerrow, K., Dorrestein, P. C., Grandy, M. R., Kelleher, N. L., El-Husseini, A., and Ting, A. Y. (2006) *Nat. Meth.* **3,** 267–273
34. Klumb, L. A., Chu, V., and Stayton, P. S. (1998) *Biochemistry* **37,** 7657–7663
35. Walstrom, K. M., Dozono, J. M., Robic, S., and von Hippel, P. H. (1997) *Biochemistry* **36,** 7980–7992
36. Walmacq, C., Rahmouni, A. R., and Boudvillain, M. (2006) *Biochemistry*

45, 5885–5895
37. Walmacq, C., Rahmouni, A. R., and Boudvillain, M. (2004) *J. Mol. Biol.* **342,** 403–420
38. Wei, R. R., and Richardson, J. P. (2001) *J. Mol. Biol.* **314,** 1007–1015
39. Wei, R. R., and Richardson, J. P. (2001) *J. Biol. Chem.* **276,** 28380–28387
40. Burgess, B. R., and Richardson, J. P. (2001) *J. Biol. Chem.* **276,** 4182–4189
41. Nowatzke, W., Richardson, L., and Richardson, J. P. (1996) *Methods Enzymol.* **274,** 353–363
42. Schwartz, A., Rahmouni, A. R., and Boudvillain, M. (2003) *EMBO J.* **22,** 3385–3394
43. Qin, P. Z., and Pyle, A. M. (1999) *Methods* **18,** 60–70
44. Persson, T., Willkomm, D. K., and Hartmann, R. K. (2005) in *Handbook of RNA Biochemistry* (Hartmann, R. K., Bindereif, A., Schön, A., and Westhof, E., eds) pp. 53–74, Wiley-VCH, Weinheim, Germany
45. Markham, N. R., and Zuker, M. (2005) *Nucleic Acids Res.* **33,** (Web Server issue), W577–581
46. Schwartz, A., Walmacq, C., Rahmouni, A. R., and Boudvillain, M. (2007) *Biochemistry* **46,** 9366–9379
47. Le Trong, I., Humbert, N., Ward, T. R., and Stenkamp, R. E. (2006) *J. Mol. Biol.* **356,** 738–745
48. Richardson, J. P. (2002) *Biochim. Biophys. Acta* **1577,** 251–260
49. Adelman, J. L., Jeong, Y. J., Liao, J. C., Patel, G., Kim, D. E., Oster, G., and Patel, S. S. (2006) *Mol. Cell* **22,** 611–621
50. Steinmetz, E. J., Brennan, C. A., and Platt, T. (1990) *J. Biol. Chem.* **265,** 18408–18413
51. Walstrom, K. M., Dozono, J. M., and von Hippel, P. H. (1998) *J. Mol. Biol.* **279,** 713–726
52. Walstrom, K. M., Dozono, J. M., and von Hippel, P. H. (1997) *Biochemistry* **36,** 7993–8004
53. Burns, C. M., Nowatzke, W. L., and Richardson, J. P. (1999) *J. Biol. Chem.* **274,** 5245–5251
54. Chalissery, J., Banerjee, S., Bandey, I., and Sen, R. (2007) *J. Mol. Biol.* **371,** 855–872
55. Eoff, R. L., and Raney, K. D. (2005) *Biochem. Soc. Trans.* **33,** Pt. 6, 1474–1478
56. Vieu, E., and Rahmouni, A. R. (2004) *J. Mol. Biol.* **339,** 1077–1087
57. Wong, S. S., Joselevich, E., Woolley, A. T., Cheung, C. L., and Lieber, C. M. (1998) *Nature* **394,** 52–55
58. Moy, V. T., Florin, E. L., and Gaub, H. E. (1994) *Science* **266,** 257–259
59. Dalal, R. V., Larson, M. H., Neuman, K. C., Gelles, J., Landick, R., and Block, S. M. (2006) *Mol. Cell* **23,** 231–239
60. Evans, E. (2001) *Annu. Rev. Biophys. Biomol. Struct.* **30,** 105–128
61. Hyeon, C., and Thirumalai, D. (2007) *Biophys. J.* **92,** 731–743
62. Greenblatt, J., and Li, J. (1981) *Cell* **24,** 421–428
63. Schmidt, M. C., and Chamberlin, M. J. (1984) *J. Biol. Chem.* **259,** 15000–15002
64. Knowlton, J. R., Bubunenko, M., Andrykovitch, M., Guo, W., Routzahn, K. M., Waugh, D. S., Court, D. L., and Ji, X. (2003) *Biochemistry* **42,** 2275–2281
65. Pasman, Z., and von Hippel, P. H. (2000) *Biochemistry* **39,** 5573–5585
66. Jin, D. J., Burgess, R. R., Richardson, J. P., and Gross, C. A. (1992) *Proc. Natl. Acad. Sci. U. S. A.* **89,** 1453–1457